Building Tomorrow's Society
Bâtir la Société de Demain

Fredericton, Canada
June 13 – June 16, 2018/ *Juin 13 – Juin 16, 2018*

DIRECT MODELLING OF DYNAMIC SOL-STRUCTURE INTERACTION BY FINITE ELEMENTS ANALYSIS

Rioux, Marc-Denis[1,6] / Nollet, Marie-José[2] / Lebœuf, Denis[3] / Koboevic, Sanda[4] / Galy, Bertrand[5]
[1] Ph.D. student, École de Technologie Supérieure (ÉTS), Canada
[2] Professor, École de Technologie Supérieure (ÉTS), Canada
[3] Professor, Laval University, Canada
[4] Professor, Polytechnique Montréal, Canada
[5] Researcher, IRSST, Canada
[6] marc-denis.rioux.1@ens.etsmtl.ca

Abstract: The objective of this paper is to investigate the impact of different types of artificial boundaries on the dynamic behaviour of a free oscillating structure founded at the surface of a soil deposit. The superstructure consists of a moment resisting frame and the soil is considered as a stress dependent medium. 24 DSSI 2D finite elements models are constructed on OpenSees platform. Beam-column elements with fibre sections, including confined and unconfined concrete and steel reinforcement, are employed to represent the frame members. Soil behaviour is modelled using an inelastic multi-yield surface material to a depth of 30 meter in total stress condition. Three different types of lateral boundaries are applied to the soil domain in order to assess their impact on the period elongation and overall damping of the structure under free vibration. Different soil width-to-depth ratios (ϖ=w/H) are considered to evaluate the influence of the distance between the lateral boundaries and the structure. The study showed that the best approach to model the artificial lateral frontier for the problem of the free vibration of a structure located at the surface of an inelastic soil domain (depth 30 meter modelled as a stress dependant medium) is the viscous lateral boundary, using large lateral distance between the structure's footing and the lateral boundary ($\varpi \geq 8$).

1 INTRODUCTION

The current engineering practice rarely considers dynamic soil structure interaction (DSSI) in the design process of new buildings. Even though DSSI is generally perceived to have a beneficial impact on seismic response of the superstructure, a controversy still exists on the subject (Mylonakis and Gazetas 2000). In recent studies, it was proposed to use DSSI in the process of seismic evaluation of existing structures as it might prevent unnecessary retrofits by reducing the seismic force applied to a structure (Gajan and Kutter 2008, Apari et al. 2017).

There are two main approaches to evaluate the impact of DSSI, the direct methods and the substructure approach (Stewart et al. 2012). Both approaches require dynamic modelling of the soil medium to obtain the foundation input motion (Mengi and Tanrikulu 1993). The proper assessment of the extent of the far field is the key aspect in the modelling of the soil. While theoretically the soil medium extend to infinity, in the context of finite element analysis it is necessary to truncated it thereby creating artificial boundaries

that do not exist in reality. The infinite soil medium is then modelled as a reduced region called the finite domain (Wolf 1985).

The artificial boundaries must prevent, or at least minimize, wave reflection back into the finite domain for the model to be of any value. This problem has been examined by Lysmer and Kuhlmeyer (1969) who proposed to add dashpot at the numerical lateral boundary to absorb incoming wave and prevent reflection back in the model. This approach can also be used to model the flexibility of the underlying soil deposit at the bottom boundary (Lysmer 1978). Another method to model the artificial boundary is the use of the periodic lateral boundary, better known as the Tied Degree Of Freedom approach (TDOF) (Zienkiewicz et al. 1989). Other methods have been proposed over the years to assess this problem. Comparisons for the efficiency of these methods applied to linear elastic or pseudo elastic soil have been published (Mengi and Tanrikulu 1993, Kontoe et al. 2007).

In the context of DSSI, where large loads are transferred from the structure to the soil, it appears crucial that the soil model be stress dependent and that correct assessment of initial state of stress be reproduced. Several reconnaissance reports show that non-linear behaviour of soil occurred during earthquake events and had a major impact on the dynamic behaviour of the supported structure in the case (Avilès and Pérez-Rocha 1998, Gajan and Kutter 2008, Giorgini et al. 2012, Raychowdhury and Singh 2012). Non-linear DSSI behaviour have been observed even under moderate shaking events (Pecker 2011). Thus, the modelling the soil as a linear elastic homogenous medium does not seem adequate. To the best of the author's knowledge, studies examining the efficiency of artificial boundaries for the problem of inelastic DSSI with a soil model that is stress dependent have not been reported in the literature.

In this paper, the impact of different types of artificial boundaries on the dynamic behaviour of a free oscillating structure founded on the surface of a 30 metres soil deposit is investigated. The soil is considered as a stress dependent medium.24 DSSI 2D finite elements models are constructed on OpenSees platform. Three different types of lateral boundaries are applied to the soil domain. Their impact on the response of the soil-structure system is traced through the period elongation and overall damping. Different width-to-depth ratios of soil medium (ϖ=w/H) are considered to evaluate the influence of the distance between the lateral boundaries and the structure.

2 METHODOLOGY

2.1 Description of the Analysis

To reach the objective, a series of 24 DSSI models are constructed using 2D finite elements. The models are developed in the free software Opensees (OS) (McKenna 1997, Mazzonial et al. 2006). Three different types of artificial lateral boundaries are applied to the soil domain in order to assess their impact on the period elongation and overall damping of the structure under free vibration. In each model, the structure considered is a 3-storey 3-bays reinforced concrete (RC) moment resisting frame 12.2m high, with exterior bay width equal to 8.5m and interior bay width equal to 3m for a total width of the structure of 20m. The frame has 4 distinct footings located at the surface of the soil deposit with dimension L=2m. This type of structure represents a common structural system build between 1960 and 1970 for institutional buildings in the province of Quebec (Lefebvre 2012). The soil considered is a sand deposit in total stress condition with a shear wave velocity (V_s) of 270 m/sec and depth (z) of 30m.

Four different ratios of soil widths to depth (ϖ=w/H) are considered to evaluate the influence of the distance between the lateral boundaries; 0.667, 2, 5.667, 8 (Figure 1 a). The width w is the distance between the structure's footing and the lateral boundary. For each value of ϖ, three different types of artificial boundaries are considered for the soil domain. The selected artificial boundaries were chosen on the basis of simplicity of implementation in a numerical finite element model in the prospect of being used in the practice. The first artificial lateral boundary used is the viscous artificial boundary (Lysmerm and Kuhlmeyer 1969) which consists of discrete elements (dashpots) added at the limits of the finite domain to absorb incoming waves and prevent them from bouncing back into the model. The second artificial boundary used is known as the Tied Degree Of Freedom (TDOF) (Zienkiewicz et al. 1989). In this

approach, equal displacements are imposed on nodes on lateral boundaries at equivalent height from the bottom boundary in their respective DOF. In the last artificial boundary used, referred to in the text as the fixed lateral boundary (FLB), all lateral nodes are simply fixed against lateral displacements. A view of the geometric aspect of the model including the soil and the structure is given in Figure 1 (a).

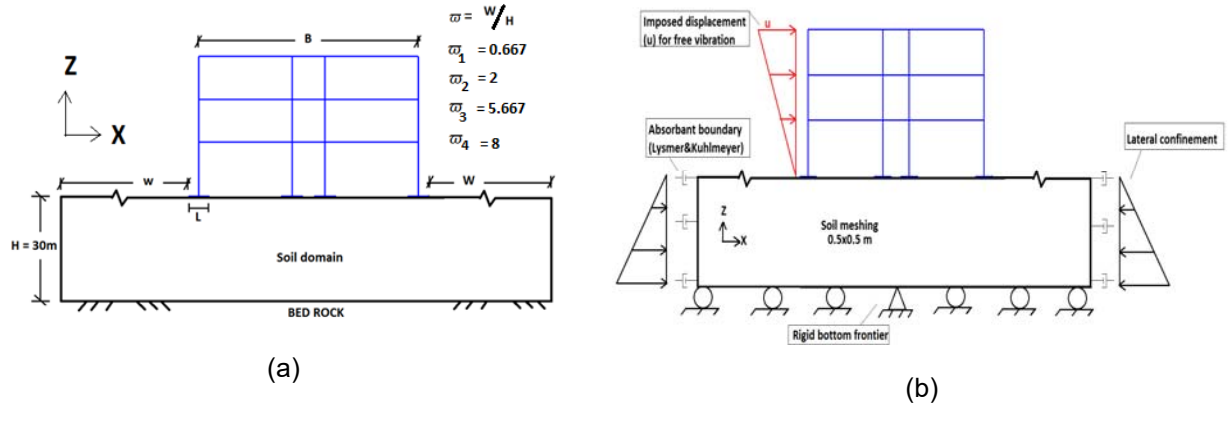

Figure 1 : (a) View of the geometric aspect of the model; (b) Schematic view of the numerical model for the case of viscous artificial lateral boundary and rigid bottom condition

For each ratio ϖ and each type of artificial lateral boundary, the bedrock rigidity is either considered infinite, as depicted in Figure 1 b), or considered finite, and represented using a series of dashpot included to the bottom's frontier nodes to account for the finite rigidity of the underlying bedrock (Lysmer 1978). Properties of bedrock used for the half-space are density (ρ) taken as 2 400 kg/m³ and shear wave velocity (V_S) taken as 760 m/sec. Table 1 resume the different models tested.

Table 1 : List of tested models and characteristic parameters

Bedrock	$\varpi = {}^{W}/_{H}$	FLB	Viscous	TDOF
Infinite rigidity	0.667	1.A.1	2.A.1	3.A.1
	2	1.A.2	2.A.2	3.A.2
	5.667	1.A.3	2.A.3	3.A.3
	8	1.A.4	2.A.4	3.A.4
Finite rigidity	0.667	1.B.1	2.B.1	3.B.1
	2	1.B.2	2.B.2	3.B.2
	5.667	1.B.3	2.B.3	3.B.3
	8	1.B.4	2.B.4	3.B.4

2.2 Numerical Modelling – Soil

The soil domain is constructed using 0.5x0.5m quadratic elements with a single stabilized gauss point (McGann et al. 2012). The soil mesh is 30 meters deep and has variable ratio ϖ of width to depth, as shown in Figure 1 a) and Table 1. Effect of passive lateral earth force on the soil domain is modelled using loads at each node of the lateral boundaries. The values of the loads to apply are obtained by recording stress in high stiffness spring attached to the artificial boundaries in the first static consolidation analysis steps. The springs are then removed and the forces recorded in each spring are applied to the associated node.

The analysis is conducted in total stress condition, i.e. pore water pressures are not considered. Soil behaviour is modelled using an inelastic multi-yield surface material of the OS library called pressureDependentMultiyield (PDMY) (Yang et al. 2003). Instead of having a single yield limit, the PDMY material defines a nested series of surface which allows representing the small strain behaviour displayed by natural soils. Figure 2 shows the series of yield limits in the principal effective stress space and in the

deviatoric plane. As can be seen, the shape of individual yield limit is similar to the Drucker-Prager yield limits (Drucker and Prager 1952).

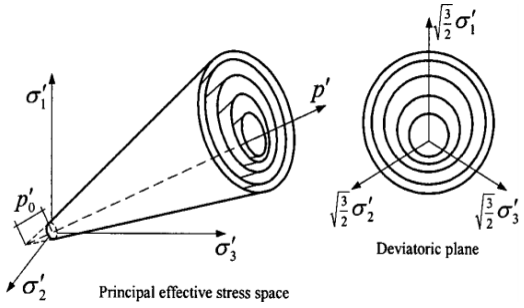

Figure 2 : Conical yield surfaces in principal stress space and deviatoric plane - (Yang et al. 2003)

Values of the soil parameters used in the PDMY model are shown in Table 2, where ρ is soil mass density, φ is the angle of friction of the soil, γ_{max} is the maximum shear strain, P_r is the reference pressure for G_{max} and K_{max}, and ν is Poisson's ratio.

Table 2 : Value of the main parameters used in definition of the PDYM material

ρ (kg/m³)	φ (°)	γ_{max} (%)	P_r (kPa)	ν
1635	37	1	101.3	0.27

The value of the small strain shear modulus G_{max} is calculated from Eq. 1 (Seed and Idriss 1970):

[1] $G_{max} = 21{,}7K_{2-max}P_{atm}\sqrt{\sigma_m'/P_{atm}}$

where P_{atm} is the atmospheric pressure (≈ 101.3kPa), σ_m' is the mean effective confining pressure, ν Poisson's ratio and K_{2-max} is a parameter establishing the link between the shear modulus value and the confinement pressure, obtained from linear interpolation between value given in the work of Seed and Idriss (1970) or in tabulated format (Kramer 1996). The value of the small strain bulk modulus K_{max} is directly obtained by Eq. 2:

[2] $K_{max} = \frac{2G(1+\nu)}{3(1-2\nu)}$

To ensure a proper choice of G_{max} considering the weight of the structure, an iterative procedure is used. Initial values for G_{max} are chosen as to obtain a V_s of 270 m/sec on the whole soil domain. Static analyses are then conducted and stress state at each element is recorded. Updated value for G_{max} & K_{max} are then computed from equations 1 and 2 and the static analysis is resumed until a stable solution is reached. During the dynamic phase of the analysis, the dependency of the soil to shear strain is directly taken into account in the PDMY material at each time steps based on a hyperbolic relation (Seed and Idriss 1970). Most models used in previous studies do not consider the initialisation of the state of stress and/or the dependency of the shear modulus to the shear strain as the soil is usually modeled as an elastic medium.

2.3 Numerical Modelling – Structure

Fibre sections, including confined and unconfined concrete and reinforcement steel are used to model the structural elements. The inelastic stress-strain relationships considered for structural elements are Concrete02 (Hisham and Yassin 1994) and Steel02 (Filippou et al. 1983) of the OS library. Although the structure remains elastic under free vibration, the non-linearity of the elements was modelled for future analyses. Concrete02 requires input of f_c', the concrete's compressive strength at 28 days, ε_{c0}, the concrete strain at maximum strength, f_{cu}', the concrete crushing strength, ε_{cu}, the concrete strain at

crushing strength, λ, the ratio between the unloading and initial slope at ε_{cu}, f_t, the tensile strength and E_{ts}, the tension softening stiffness. Steel02 requires input of f_y, the yield strength, E_0, the initial elastic tangent, b, the strain-hardening ratio and parameter to control the transition to plastic branches (R0, CR1, CR2) as well as an optional isotropic hardening parameter. Details about the values used for these parameters and other structural considerations can be found in Apari-Lauzier (2016).

2.4 Free Vibration Analysis

Free vibration of the structure is initiated by a small displacement applied on the left of the frame in accordance with the first modal shape with maximal amplitude of 10^{-6} m. The motion of the top left node of the structure is then recorded and the displacement relative to the base of the footing displacement is calculated. No slipping or uplifting is considered on the interfaces between the soil and the four footings. Numerical period is taken as the mean value obtained between several peaks of the recorded relative displacement. It is then compared with the theoretical value obtained for the classical case of a single degree of freedom (SDOF) elastic oscillator with horizontal, vertical and rotation spring. Theoretical elongation of the SDOF elastic oscillator is given by Eq. 3 (Stewart et al. 2012, Veletsos and Meek 1974):

$$[3]\ \frac{\hat{T}}{T} = \sqrt{1 + \frac{k}{k_x} + \frac{kh^2}{k_{yy}}}$$

where $\hat{T}$ is the natural period of the structure on a flexible base, T is the natural period of the structure on a fixed base, k the rigidity of the structure, k_x the dynamic stiffness of the horizontal spring, k_{yy} the rotational stiffness and h the height of the SDOF model (≈2/3 Height of the structure). The logarithm decrement method, Eq. 4 (Paultre 2005), is used to estimate the damping of the structure (β) during the free vibration:

$$[4]\ \xi \approx \frac{\delta_m}{2\pi} = \frac{1}{2\pi m} \ln\left[\frac{u_n}{u_{n+m}}\right]$$

where u_n is the displacement at cycle n and u_{n+m} is the displacement after m additional cycles. Values of damping obtained are compared with theoretical values expected for the case of a flexible base structure with consideration of foundation damping (β_f) (Stewart et al. 2012):

$$[5]\ \beta = \beta_f + \frac{1}{(\hat{T}/T)^n}\beta_i$$

where β_i is the structural damping for the structure considering fixed base condition and exponent n is taken as 3 for linearly viscous structural damping and 2 otherwise (Stewart et al. 2012). The development of Eq. 3 and Eq. 5 are based on the hypothesis of a SDOF elastic system built over an elastic infinite domain. Since the shape of the imposed displacement respect the first modal shape of the structure and that displacement in both the structure and the soil remains very small, the test conditions for the numerical DSSI finite element model are close to those used in the derivation of the theoretical relation. Hence Eq. 3 and Eq. 5 will serve as benchmark to evaluate the efficiency of the evaluated models presented in Table 1.

3 NUMERICAL RESULTS

In each analysis given in Table 1, the free oscillation is recorded during a 2.5 s interval. Time steps are approximately 0.0005 s with 5000 steps considered in each model. Figure 3 shows an example of the relative lateral displacement of the left top corner of the frame. Damping and difference between

numerical and theoretical ratios of period elongation for all models are presented in

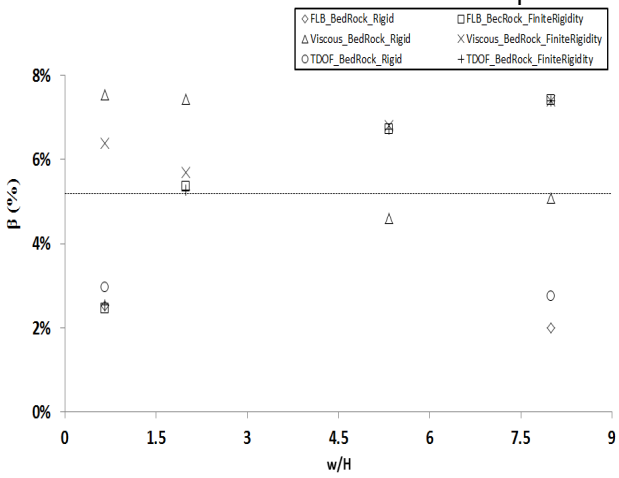

Figure 4.

Numerical results of models with fixed lateral boundaries and rigid bedrock and increasing value of the ratio ϖ (1.A.1, 1.A.2, 1.A.3 and 1.A.4) are shown in Figure 3 a). They indicate that increasing the value of the ratio ϖ, in other words, increasing the distance between the lateral boundaries, have a significant impact on the recorded displacements. In model 1.A.1 (ϖ = 0.667), the displacement shows a transitory phase followed by a smooth permanent phase with damping ≈1.7%. In model 1.A.2 (ϖ = 2), following the transitory phase, the model fails to develop a smooth permanent phase, as shown by the failed peak at 0.5 s. Model 1.A.3 (ϖ = 5.667), develops a similar trend. Model 1.A.4 (ϖ = 8), develops a permanent phase but the permanent variation in amplitude shows that the motion is perturbed. Estimation of periods or damping from models 1.A.2 and 1.A.3 is irrelevant. Pattern displayed by these models indicates that an incoming wave disrupted the free vibration of the building. Since all movements originate from the structure, the disturbance is an effect of the boundary, lateral and/or bottom.

Results from models with FLB and finite rigidity of the bedrock and increasing value of the ratio ϖ (1.B.1, 1.B.2, 1.B.3 and 1.B.4) are shown in Figure 3 b). After the initial transitory phase, the model develops in each case a smooth permanent shape. However, damping differs greatly. Model 1.B.1 (ϖ = 0.667) displays a damping ≈2,25% whilst models 1.B.2 (ϖ = 2), 1.B.3 (ϖ = 5.667) and 1.B.4 (ϖ = 8) display increasing level of damping with increasing value of ϖ , from 4.5% for model 1.B.2 to 7.4% for model 1.B.4. This trend indicates that in model 1.B.1, the lateral boundary of the model is close enough to limit the impact of the finite rigidity of the bedrock. In model 1.B.2, lateral boundaries are farther from the structure, thus the impact of the finite rigidity of the bedrock increases leading to an increase in the damping value.

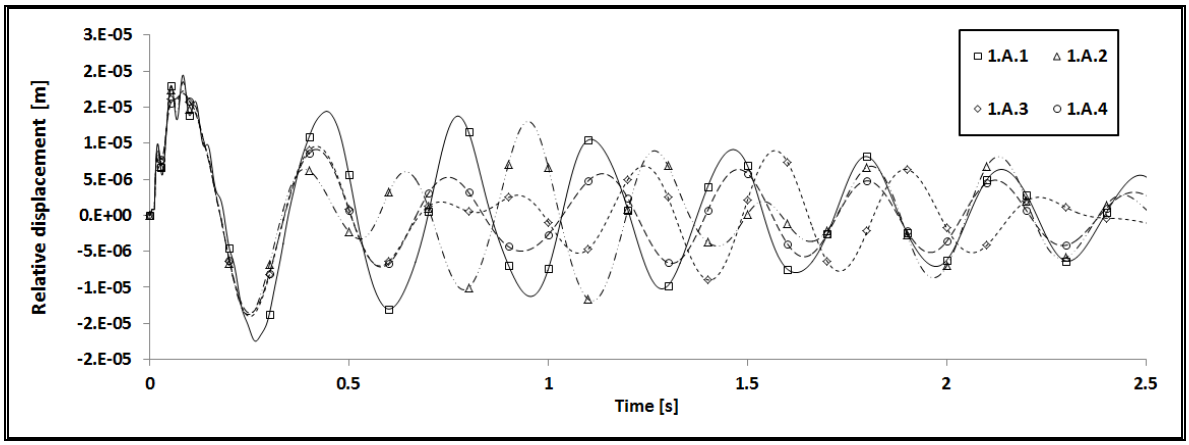

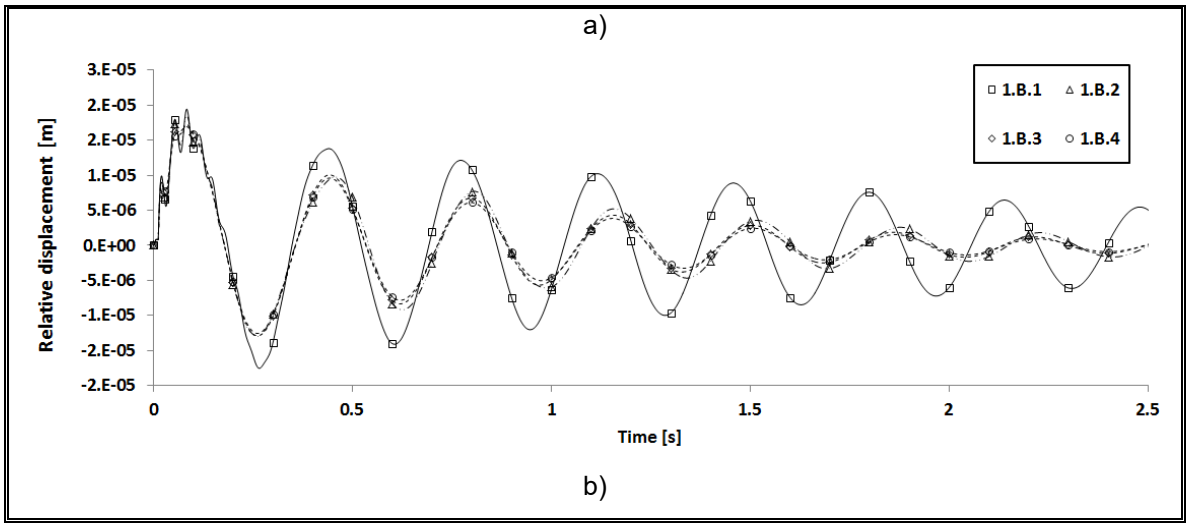

Figure 3 : Relative displacement of the top left node of structure for the case of FLB: a) rigid bedrock b) bedrock with finite rigidity (see Table 1)

Results of models with viscous lateral boundaries and rigid bedrock and increasing value of the ratio ϖ (2.A.1, 2.A.2, 2.A.3 and 2.A.4) show, independently of the value of ϖ, an initial transitory phase followed by a smooth permanent decay of the movement. Differences between the models are noted when examining their respective level of damping and period elongation. Model 2.A.1 (ϖ = 0.667) has higher damping than 2.A.2 (ϖ = 2) which in turn has higher damping than 2.A.3 (ϖ = 5.667). However, damping of model 2.A.4 (ϖ = 8) is higher than damping of model 2.A.3. It was expected that damping would decrease with increasing value of ϖ until a stable value was reached, as distance between the lateral dashpot and the structure is increased. When checking the ratio of period elongation, it is observed that the discrepancy between the theoretical value and the numerical value decreases with increasing ϖ, from 11.3% for model 2.A.1 to approximately 5% for model 2.A.4.

Results of models with viscous lateral boundaries with finite rigidity of the bedrock and increasing value of the ratio ϖ (2.B.1, 2.B.2, 2.B.3 and 2.B.4) are similar to results obtained from models with rigid bedrock. Again, the trend does not seem to be much influenced by ϖ. However, when comparing the elongation ratio, the discrepancy between theoretical and numerical is higher than in the viscous model with rigid bedrock. The difference in elongation ratio increases with increasing value of ϖ in all models except for 2.B.4 (ϖ = 8), remains relatively stable (+0.35%). When considering the damping, the impact of the finite rigidity of the bedrock appears. As value of ϖ increases damping increases and reaches the same value as in model 1.B.4 (ϖ = 8), around 7.4%.

Results of models with TDOF lateral boundaries and rigid bedrock and increasing value of the ratio ϖ (3.A.1, 3.A.2, 3.A.3 and 3.A.4) are similar, in shape, to those obtained for the case of FLB. For model 3.A.1 (ϖ = 0.667), the initial transitory phase is followed by a smooth decay in movement. Models 3.A.2 (ϖ = 2) and 3.A.3 (ϖ = 5.667) however, fail to develop a smooth permanent phase, similar as what was observed with models 1.A.2 and 1.A.3. This suggests, again, that an incoming wave did impact the movement. Model 3.A.4 (ϖ = 8) develops a seemingly permanent phase, although the pattern is less influenced by wave reflection than model 1.A.4. Period elongation ratio and damping for model 3.A.2 and 3.A.3 were not computed as the displacement pattern was irrelevant. When comparing the elongation ratio for model 3.A.1 and 3.A.4, very little variation is observed (+0.55%). The same pattern is seen on the level of damping, which is stable around 2.8%.

Results of models with TDOF and finite rigidity of the bedrock and increasing value of the ratio ϖ (3.B.1, 3.B.2, 3.B.3 and 3.B.4) all show an initial transitory phase followed by a smooth permanent movement. From the result, it is seen that the ratio of period elongation is little influenced by increasing value ϖ. This is not true, however, for the damping, which increases with increasing value of ϖ. For model 3.B.4 (ϖ =

8), the level of damping is roughly equal to that of model 2.B.4 (ϖ = 8), indicating that the impact of the boundary on the response is predominantly coming from the bottom frontier.

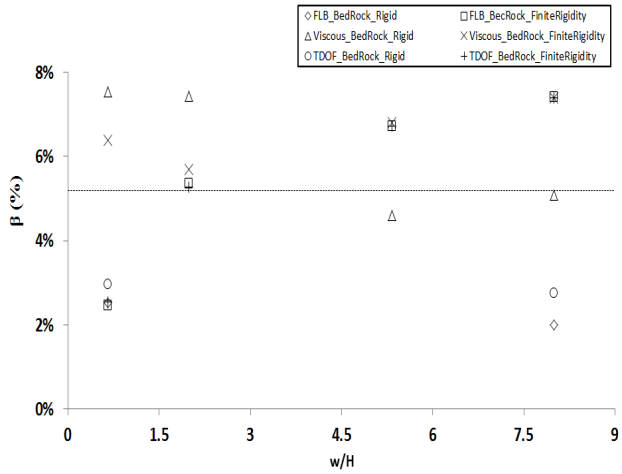

Figure 4 summarizes the values of damping for all models obtained from logarithm decrement of the relative displacement curves (Eq. 2). It can be seen that when the finite rigidity of the bedrock is modelled along with a very large soil domain on each side of the building, the damping values for all types of lateral boundaries tend to increase. When the bedrock is considered rigid, only the viscous artificial lateral boundaries does perform well, with larger value of soil domain leading close to the expected value of damping for this flexible base system.

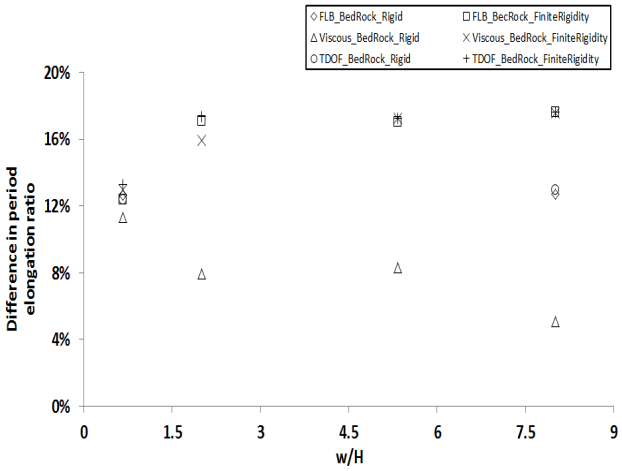

Figure 5 summarizes the values of the difference between theoretical and numerical ratios of period lengthening. As it can be seen, increasing the value of ϖ did impact the values. When the bedrock was considered rigid, the ratio did not change for the TDOF lateral boundaries. The ratio decreases in the case of the viscous lateral boundaries. When the finite rigidity of the bedrock was modelled, all types of models converged with increasing value of width up to a maximum of about 7.6%.

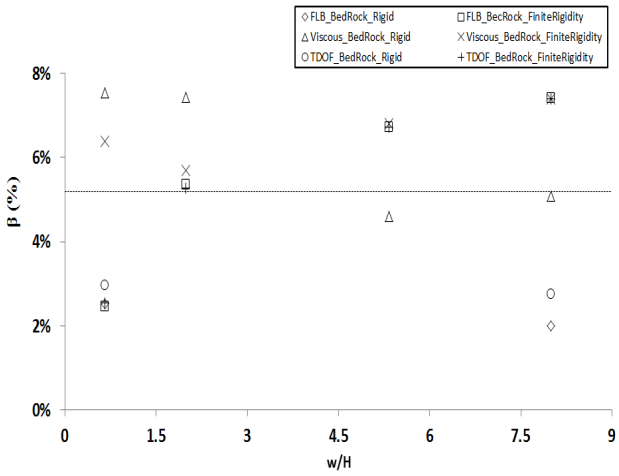

Figure 4 : Damping from logarithm decrement for the different models tested

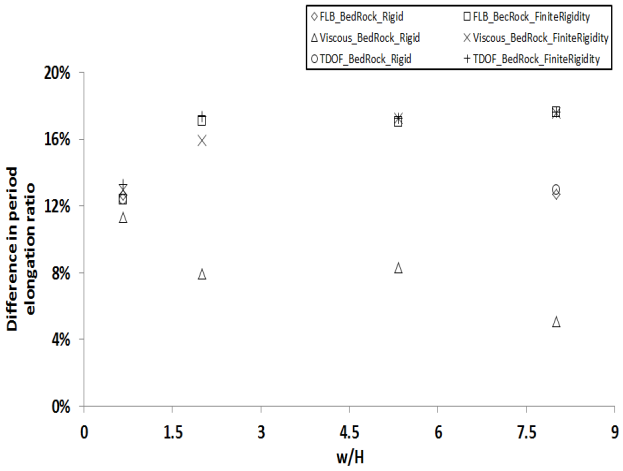

Figure 5 : Difference between theoretical and numerical ratios of period lengthening

When the result of the damping and of the difference between theoretical and numerical ratios of period lengthening are considered together, the following observations can be drawn:

- Fixed lateral boundaries performed poorly with increasing value of ϖ, or the distance between the lateral boundaries, when the bedrock was assumed rigid;
- When the finite rigidity of the bedrock was modelled, FLB period lengthening ratios were between those obtained by the viscous and TDOF methods for all values of ϖ assessed, whilst the damping value was similar for all three methods;
- Viscous lateral boundaries with rigid bedrock over damped the model with low value of ϖ. With larger value of ϖ, the method gave the best damping level of all approaches tested as well as the lowest difference between expected and numerical ratios of period lengthening;
- TDOF lateral boundary with rigid bedrock performed poorly with increasing value of ϖ;
- When the finite rigidity of the bedrock was modelled, the TDOF lateral boundary approach gave the same level of damping and of period lengthening as the FLB.

The viscous lateral boundaries with the ratio $\varpi = 8$ and rigid bedrock assumption did perform better than any other approach tested for the problem considered here. For the largest value ϖ, the difference with the expected ratio of period lengthening is ≈5% whilst the value of damping is within 1% of the expected value for this flexible base system.

4 CONCLUSION

2D finite element simulations were carried out to investigate the impact of different type of artificial boundaries on the dynamic behaviour of a free oscillating structure founded at the surface of a soil deposit modelled as a stress dependent medium. 24 DSSI models were evaluated for different type of artificial lateral boundary and different ratio of soil width to soil height. Original aspect of the work include assessment of the impact of the initial state of stress in the soil deposit on the value of the small strain shear modulus and the consideration of the shear strain on the evolution of the shear modulus during each analysis steps.

The results show the best approach to model the artificial lateral frontier for the problem of the free vibration of structure located at the surface of an inelastic soil domain of depth 30 meter modelled as a stress depend medium is the viscous lateral boundary, using large lateral distance between the structure's footing and the lateral boundary. This method shows good agreement with expected value of damping with larger value of the ratio ϖ while at the same time having good agreement with theoretical ratio of period elongation. The two other approaches valuated showed increasing gap between theoretical and numerical period elongation ratio as the ratio ϖ increased.

Acknowledgements

The financial support of the Fond Québécois Recherche sur la Nature et les Technologies (FRQNT) and the Centre d'Études Interuniversitaire des Structures sous Charges Extrêmes (CEISCE) is gratefully acknowledged.

References

Apari-Lauzier, J.-S. (2016). L'impact de l'interaction sol-structure sur l'évaluation sismique des cadres rigides en béton armée existants situés dans l'est du Canada. École Polytechnique of Montreal, Master thesis.

Apari, J.-S., Koboevic, S., and Nollet, M. J. (2017). Impact of soil-structure interaction effects on seismic assesment in moderate seismic zones. *16th World Conference on Earthquake Engineering*, Santiago, Chile.

Avilès, J. and Pérez-Rocha, L. E. (1998). Site effects and soil-structure interaction in the valley of Mexico. *Soil Dynamics and Earthquake Engineering* 17(1): 29-39.

Drucker, D. C., and Prager, W. (1952). Soil mechanics and plastic analysis for limit design. Quarterly of Applied Mathematics, 10(2), 157-165.

Filippou, F. C., Popov, E. P and Bertero Vitelmo V. (1983). Effects of bond deterioration on hysteretic behavior of reinforced concrete joints. Berkeley, Calif: Earthquake Engineering Research Center, University of California.

Gajan, S. and Kutter, B. L. (2008). Capacity, Settlement, and Energy Dissipation of Shallow Footings Subjected to Rocking. *Journal of geotechnical and geoenvironnemental engineering* 134(8): 1129-1141.

Giorgini, S., Cubrinovski, M., Pampanin, S., Carr, A. J., and Moghaddasi, M. (2012). Integrated foundation-structure modelling of a case study from the Christchurch 2011 earthquake. *15th World Conference on Earthquake Engineering*.

Hisham, M. and Yassin, M. (1994). Nonlinear Analysis of Prestressed Concrete Structures under Monotonic and Cycling Loads, University of California, Berkeley. Ph.D. thesis.

Kontoe, S., Zdravkovic, L., Potts, D. M., and E. Salandy, N. (2007). The use of absorbning boundaries in dynamic analyses of soil-structure interaction problems. *4th International Conference on Earthquake Geotechnical Engineering*, Thessaloniki-Greece.

Kramer, Steven Lawrence. (1996). *Geotechnical earthquake engineering*. Upper Saddle River, N.J.: Prentice Hall.

Lefebvre, K. (2012). Etude du comportement sous charges laterales des ossatures de beton arme avec murs de remplissage de maconnerie, construites avant les annees 1960. (Doctorat), École de technologie supérieur, Montréal, Canada.

Lysmer, J. (1978). *Analytical procedures in soil dynamics*. Berkeley: College of Engineering, University of California.

Lysmerm, J. and Kuhlmeyer, R. L. (1969). Finite Dynamic Model for Infinite Media. *Journal of the Engineering Mechanics Division* 95(4): 859-878.

Mazzoni, S., McKenna, F. T., Scott, M., and Fenves, G. L. (2006). Open System for Earthquake Engineering Simulation (Opensees). Pacific Earthquake Engineering Research Center (PEER), University of California, Berkeley, CA.

McGann, C., Arduino, P. et Mackenzie-Helnwein, P. (2012). Stabilized single-point 4-node quadrilateral element for dynamic analysis of fluid saturated porous media. *Acta Geotechnica*, vol. 7, no 4, p. 297-311.

McKenna, F. T. (1997). Object-Oriented Finite Element Programming: Frameworks for Analysis, Algorithms and Parallel Computing. Civil Engineering, University of California, Berkeley. Ph.D. thesis
Mengi, Y., & Tanrikulu, A. K. (1993). Absorbing Boundary Conditions in Soil-Structure Interaction Analyses. In P. Gülkan & R. W. Clough (Eds.), Developments in Dynamic Soil-Structure Interaction (pp. 111-146). Dordrecht: Springer Netherlands.
Mylonakis, G. and Gazetas, G. (2000). Seismic soil-structure interaction: beneficial or detrimental? *Journal of Earthquake Engineering* 4(3): 277-301.
Paultre, P. (2005). Dynamique des structures - application aux ouvrages de génie civil.
Pecker, A. (2011). Influence of non linear soil structure interaction on the seismis demand in bridges. *International conference on Innovations on Bridges and Soil-Bridge Interaction*. Athens.
Raychowdhury, P. and Singh P. (2012). Effect of nonlinear soil-structure interaction on seismic response of low-rise SMRF buildings. *Earthquake Engineering and engineering vibration* 4(11).
Seed, H. B., Idriss, I. M. (1970). Soil moduli and damping factors for dynamic response analyses. Report No. EERC 70-10, Earthquake Engineering Resource Center, University of California, Berkley, California.
Stewart, J., Crouse, C.B., Hutchinson, T. C., Lizundia, B., Naeim. F and Ostadan F.. 2012. Soil-Structure Interaction for Building Structures. National Earthquake Hazards Reduction Program.
Veletsos, A. S. and Meek, J. W. (1974). Dynamic behaviour of building-foundation systems. *Earthquake Engineering & Structural Dynamics* 3(2): 121-138.
Wolf, J. P. (1985). Dynamic soil-structure interaction: Prentice-Hall.
Yang, Z., Elgamal, A., and Parra, E. (2003). Computational Model for Cyclic Mobility and Associated Shear Deformation. *Geotechnical and Geological Engineering*, 129(12), 1119-1127.
Zienkiewicz, O. C., Bicanic, N., and Shen, F. Q. (1989). Earthquake Input Definition and the Trasmitting Boundary Conditions. In I. S. Doltsinis (Ed.), *Advances in Computational Nonlinear Mechanics* (pp. 109-138). Vienna: Springer Vienna.